Modelling gas flow undergoing phase change for investigating liquid loading in gas wells

Amieibibama Joseph
Department of Petroleum & Gas Engineering, University of Port Harcourt, Nigeria

Abstract—Production from gas wells at inception is usually a single-phase gas flow. However, pressure decline below the dew-point results in gas expansion triggering cooling and thus, the emergence of two-phase gas-liquid flow. The condensation and gradual buildup of liquids is termed liquid loading in gas wells. The rate of liquid dropout depends on several factors such as geometry of the well, the fluid composition, the type of gas reservoir and the operating conditions of the well. The occurrence of two-phase flow makes it difficult to efficiently produce gas wells when flow conditions deteriorates. This work numerically investigates a steady-state gas flow behavior undergoing a phase change by monitoring temperature, pressure, velocity and density. It was observed that decrease in temperature and pressure results in expansion of the gas, and thus cooling which leads to condensation of the liquid phase, thus increasing the liquid density. The model was validated using published experimental data and a commercial software, NIST RefProp; and the results show good agreement. With this model, the behavior of multicomponent systems undergoing phase change can be understood to prevent and mitigate excessive accumulation of liquids in gas wells that can pose potential threats to effective gas production.

Index Terms— gas-flow, liquid dropout, phase change, single phase

1 INTRODUCTION

Natural gas can occur as either a conventional or unconventional resource. The conventional natural gases are those found in underground hydrocarbon reservoirs while those found within tight pore spaces such as coal-beds and shales are termed unconventional natural gases. Production from conventional gas reservoirs will be subject of discuss in this paper. Conventional gas reservoirs can be classified in terms of their fluid properties and their initial reservoir pressure and temperature on a typical (p-T) phase diagram. Hence, gas reservoirs can be classified as either wet gas, gas-condensate or dry gas reservoirs respectively. A wet gas reservoir is a gas reservoir that has gas-oil ratio (GOR) between 60,000 to 100,000 scf/STB and whose initial reservoir temperature is above the cricondentherm "[1], [2]". Upon depletion, a wet gas well would release substantial heavier hydrocarbon fractions as temperature and pressure drops along the production path. For a retrograde gas-condensate reservoir to occur, the temperature and pressure of that reservoir must fall between the cricondentherm and critical temperature. Typical GOR of gas-condensate reservoir is between 8,000 to 70,000 scf/STB. For such reservoirs, flow would initially be single-phase gas but will inadvertently become two-phase flow once the pressure falls below the dew-point. Production from a dry gas reservoir may not result in the condensation of condensable liquids at atmospheric condition, howbeit, can release infinitesimal amount of liquids at pressures much lower than the atmospheric pressure at separator conditions [1]. Depending on the operating conditions of a well and the inherent fluid composition, there is the tendency for a single-phase flow to degenerate to a two-phase flow. In this paper, modelling approach is adopted to investigate the flow behavior of an initially single-phase flow system undergoing phase change as temperature and pressure changes in the well.

2 METHOD

The first step towards understanding this process is to develop a model to simulate gas flow without phase change and then extend it to phase change. The following simplifying assumptions were made:

1. A constant mass flow rate was assumed.
2. The wellbore was assumed to have constant cross-sectional area.

2.1 A Single-Phase Gas Flow Model

Above the dew-point, a single-phase model is most appropriate to model gas flow. Four variables were considered for the numerical simulation: temperature T; velocity v; density ϱ and pressure p, hence four ordinary differential equations are required. These are the conservation of energy, mass and momentum equations and the gas law as the equation of state. Flow was considered to be in the positive z -direction starting with at $z = 0$.

The energy conservation equation is expressed as [3,4]:

$$H + \frac{v^2}{2} + gz = \text{constant}, \qquad (1)$$

where H, is the specific enthalpy, v is the velocity and g is the acceleration due to gravity. Considering fluid flow up the wellbore, Equation 1 was differentiated with respect to z,

$$c_p \frac{dT}{dz} + v\frac{dv}{dz} + g = 0, \quad (2)$$

here $dH = c_p dT$, c_p is the specific heat capacity at constant pressure, and T is the temperature.

The mass conservation equation is expressed as:

$$\frac{d(\rho v)}{dz} = 0. \quad (3)$$

Hence, the mass flow rate per unit area, $\rho v =$ constant, thus:

$$\rho\frac{dv}{dz} + v\frac{d\rho}{dz} = 0. \quad (4)$$

The conservation of momentum equation is expressed as:

$$\frac{d\sigma}{dz} + \rho g = \rho v\frac{dv}{dz}, \quad (5)$$

where σ is the stress (tension taken as positive), g is the acceleration due to gravity. The system of ordinary differential equations is closed with the gas law for real gases:

$$pV = ZnRT \quad (6)$$

where $\hat{R} = R/m$, is the specific gas constant and m is the molecular mass. Differentiating Equation 6 with respect to z gives:

$$\frac{dp}{dz} - Z\hat{R}T\frac{d\rho}{dz} - Z\hat{R}\rho\frac{dT}{dz} = 0. \quad (8)$$

The Peng-Robinson equation of state, was used to determine the value of Z. A Matlab program was developed to numerically analyze this model. The code was also tested using parameter values appropriate for methane, and the results were validated against published experimental data at the results and discussion session.

2.3 Two-Phase Real Gas Flow Model

Following the validation of the single component single-phase real gas flow model, the model was modified to a two-phase real gas flow model. In this model, the liquid is assumed to be carried as a mist by the gas during flow.

For a two-phase flow of a single compressible hydrocarbon fluid, six variables: temperature, pressure, density of the mixture ρ_m, density of the liquid phase ρ_l, density of the vapour phase ρ_g, and the mixture velocity v are required instead of four. Solution of this model requires six independent equations. These include: a mass and momentum conservation equations similar to Equations 4 and 5 for each phase but the density is replaced with the density of the mixture ρ_m, in this model. A combined energy equation for the mixture and the Peng-Robinson Equation of State was also used.

$$\frac{d}{dz}\left[\rho_g v\left(H_g + \frac{v^2}{2} + gz\right)\right] + \frac{d}{dz}\left[\rho_l v\left(H_l + \frac{v^2}{2} + gz\right)\right] = 0. \quad (9)$$

Here, H_g and H_l are the specific enthalpies for the gas and liquid phases. The specific enthalpy for each phase was determined using Equation 23 from the Peng-Robinson paper [5] and reproduced here as:

$$H - H^* = RT(Z-1) + \left(\frac{1}{2\sqrt{2b}}\right)\left(T\frac{da}{dT} - a\right)\left(\frac{Z + 2.414B}{Z - 0.414B}\right) = 0. \quad (10)$$

where H^* is the specific enthalpy of an ideal gas at temperature T and pressure p. In this work, the specific enthalpy of the ideal gas H^*, was calculated using the Fouad and Lloyd [6] correlation:

$$H^* = BT + CT\left(\frac{D}{T}\right)coth\left(\frac{D}{T}\right) - ET\left(\frac{F}{T}\right)tanh\left(\frac{F}{T}\right) + A \quad (11)$$

Here A, B, C, D, E, and F are constants which can be obtained from tables. The Fouad and Lloyd correlation is used because of its accuracy and simplicity in application. The remaining three equations that completes the ordinary differential equations are obtained from a combined fugacity equation Equations (12a) and (12b),

$$\ln\left(\frac{f_k^l}{x_k^l p}\right) = \frac{b_k}{b}(Z^l - 1) - \ln(Z^l - B) - \frac{A}{2\sqrt{2B}}\left(\frac{2\sum_{i=1}^{N} x_i a_{ik}}{a} - \frac{b_k}{b}\right)\ln\left(\frac{Z^l + 2.414B}{Z^l - 0.414B}\right) \quad (12a)$$

$$\left(\frac{f_k^v}{x_k^v p}\right) = \frac{b_k}{b}(Z^v - 1) - ln(Z^v - B) - \frac{A}{2\sqrt{2B}}\left(\frac{2\sum_{i=1}^{N} x_i a_{ik}}{a} - \frac{b_k}{b}\right)ln\left(\frac{Z^v + 2.414B}{Z^v - 0.414B}\right) \quad (12b)$$

and Equation 13 which was used to determine the compressibility factor for the phases

$$Z^3 - (1-B)Z^2 + (A - 3B^2 - 2B) - (AB - B^2 - B^3) = 0 \quad (13)$$

where

$$Z = \frac{pV}{RT} \quad (14)$$

$$A = \frac{ap}{R^2T^2} \quad (15)$$

$$B = \frac{bP}{RT} \quad (16)$$

Here, a and b are parameters defined in the Peng and Robinson (1976) paper. Dynamic equilibrium was assumed throughout the process, hence the Gibbs energy is the same in the liquid and vapour phases at any stage of the process. As the mass fraction of both the liquid and gas change during this process, that was also tracked and the sum of the liquid and gas mass fractions equal unity. This model was also tested using parameter values appropriate for methane and the results compared with published data in the results and discussion section.

3. Solution Method

From each scenario investigated, systems of ordinary differential equations (ODEs) were developed and solved. A fourth/fifth-order explicit Runge-Kutta method, is used in which the dependent variables of the differentials are placed on the left-hand side and all other coefficients and expressions are placed on the right-hand side of the equation. This arrangement gae rise to the linear system of ordinary differential equations:

$$[A_m]\frac{d}{dz}[X] = [b_m] \quad (17)$$

4. Results & Discussions

In the development of the single component real gas flow

model, phase change was not considered and the parameters of pure methane were used since these are readily available in published literatures. The initial values were arbitrarily chosen, although values slightly above the critical conditions of methane were used. This is because for pure substance like methane, at temperatures greater than the critical temperature, liquid and vapour phases cannot both exist in equilibrium; likewise, at pressures above the critical pressure, liquid and vapour will not coexist at equilibrium [7]. The flowing gas was given an initial temperature of 200 K, an initial pressure of 6.9 MPa and an initial velocity of 0.001 m/s. The initial density of the gas was determined using the real gas equation of state, Equation 7, with the compressibility factor Z, determined using Equation 13. Figure 1 illustrates how these variables alter as the gas flows up the production tubing given three different initial temperatures. As can be seen in Fig. 1, the gas expands as the pressure declines which causes the density to decrease. To maintain a constant mass flow rate with this decreasing density, the velocity increases. This expansion causes cooling, so the temperature declines; while the decreasing density results in the gas exerting less pressure. A sensitivity analysis was carried out to investigate the impact of variations of temperature and pressure on the flow variables; and similar trends were observed across the length of the pipe investigated as in the base case.

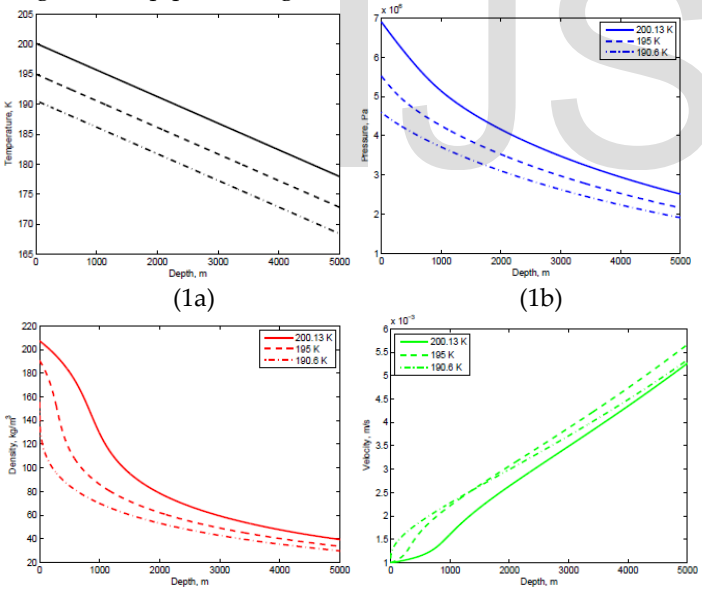

Fig. 1: profiles of (a) Temperature, (b) Pressure, (c) Density and (d) velocity against depth for pure methane not undergoing phase change

The mass and the energy determined during the simulation were checked to ensure that the model correctly predicted constant mass flow rate and that energy is conserved as shown in Fig. 2. Fig. 2(a) shows that the real gas law is satisfied with a value of approximately zero, Fig. 2(b) shows a constant mass flux per unit area, while Fig. 2(c) shows that the specific energy is also conserved during flow; both having small relative errors. Fig. 3 shows an isothermal pressure-volume (pV) plot for methane which is produced using the convhull function and the Helmholtz energy. The blue thick isotherm shows the expansion of pure methane flowing up the tubing as the pressure decreases at a temperature of 200 K, while the thin red dots are isotherms of methane at different temperatures. The different isotherms show how the volume occupied by the gas increases as the pressure decreases.

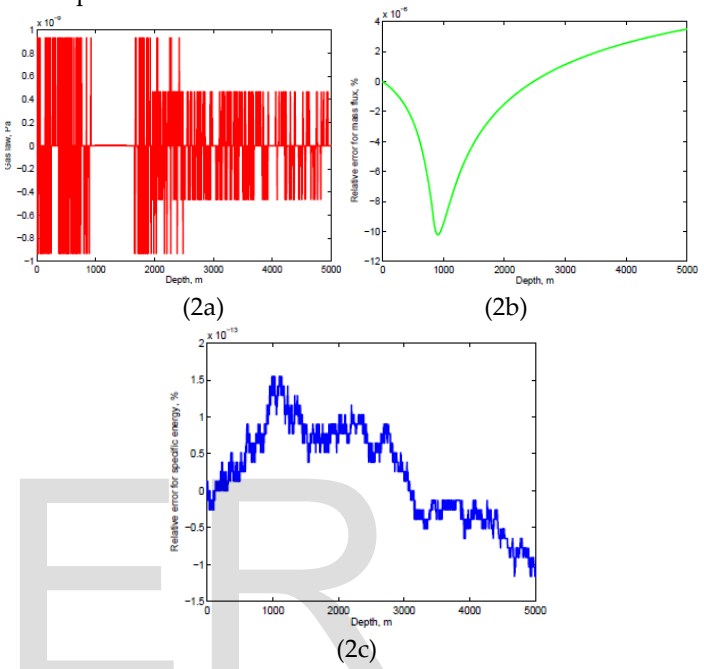

Fig. 2: Numerical validation showing that conservation laws are obeyed for single-component single phase real gas flow. (a) Real gas law ($p - \rho ZRT = 0$), is constant, (b) relative error for mass flux $\left[\left((\dot{m}(z) - \dot{m}(0))/\dot{m}(0)\right) \times 100\right]$, is constant and (c) relative error for specific energy $\left[\left(\left(\dot{E}(z) - \dot{E}(0)\right)/\dot{E}(0)\right) \times 100\right]$, is constant from the bottom of the wellbore to the top.

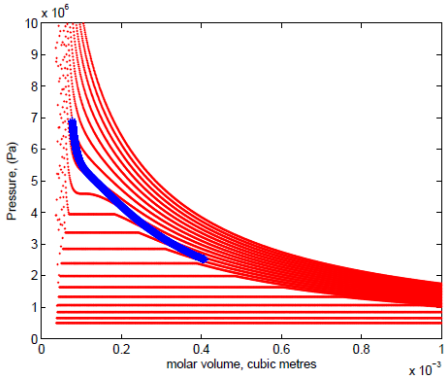

Fig. 3: pressure versus molar volume plot showing (as a thick blue line) the path of methane expanding as the pressure declines at a temperature of 200K and a starting pressure of 6.9MPa. Isotherms for methane are shown as red dots.

Fig. 4 shows a comparison of the simulation results with experimental data obtained from Setzmann and Wagner [8]. Fig. 4(a) shows the vapour pressure curve for pure methane showing the

critical point (C). The vapour-pressure curve shown in Fig. 4(a) represents the dewpoint and bubble-point curves, each lying on each other. For a pure substance, as in this case, the vapour-pressure curve also represents the transition boundary between the liquid phase and vapour phase. As can be seen in Fig. 4(a), the result from the simulation is in good agreement with the experimental data. Fig.s 4(b) and 4(c) show the effect of decreasing temperature and pressure on the density of pure methane as it expands up the pipe. The density of the gas also decreases as the pressure and temperature decreases and this is also in good agreement with the experimental data.

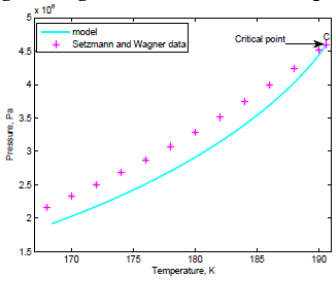

(4a)

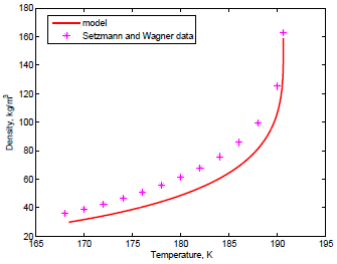

(4b)

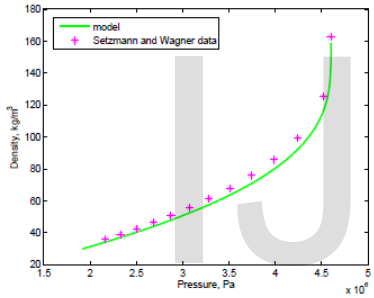

(4c)

Fig. 4: validation of simulation results for pure methane (a) plot of pressure versus temperature showing the vapour pressure line, (b) plot showing the variation of density with temperature for pure methane, (c) plot showing the variation of density with pressure for real gas flow of pure methane. The magenta asterisk are experimental data points from Setzmann and Wagner (1991).

Single-component two-phase real gas flow model with phase change

Following the successful validation of the single component real gas flow model without phase change, the model was extended to a single component two-phase flow where phase change is considered. Fig. 5 is an isothermal pressure-volume (pV) plot that shows the behaviour of pure methane undergoing a phase change.

The initial temperature was set at 185.6 K, below the critical temperature with a start pressure of 3.951 MPa that placed the initial values correctly within the two-phase region of the pV plot. The initial mass fraction of the gas was set at 0.5 and the molar volume of the mixture as the pressure declines is shown as the thick green line. The molar volume of the liquid phase (shown as the thick blue line) and that of the vapour phase (the thick cyan line); both follows the correct path on the pV plot. Again, the mass flow rate and the energy were also checked to ensure that they remain constant and this is shown in Fig. 6. From Fig.s 6(a) and 6(b), it can be seen that the mass flux per unit area and the specific energy per unit area are constant, having approximately zero percent relative errors from the bottom of the wellbore to the top of the pipe.

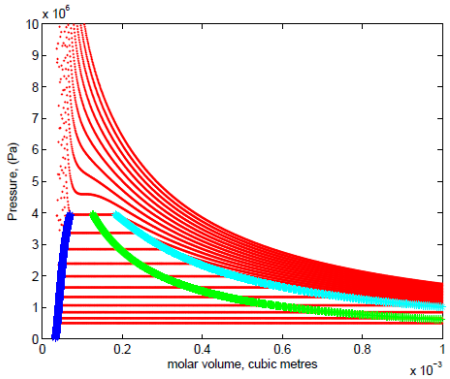

Fig. 5: Pressure-volume diagram of a single component methane undergoing phase change. The molar volume of the liquid-vapour mixture expanding as it travels up production tubing from an initial temperature of 185.6 K and 3.951 MPa is shown as thick green line. The saturated liquid phase is shown as the thick blue line while that of the saturated vapour phase is shown as the thick cyan line. Isotherms for methane are shown as red dots.

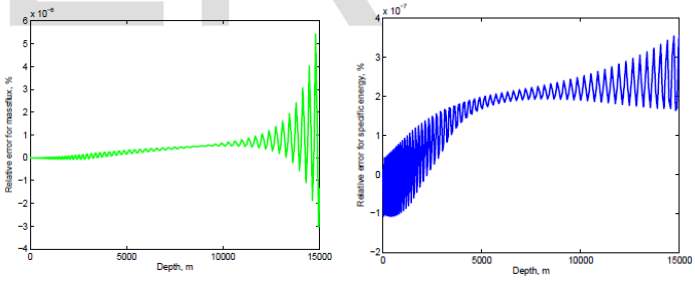

(6a) (6b)

Fig. 6: Numerical validations showing that mass and energy are conserved during the simulation of a single-component two-phase compressible flow. (a) relative error for mass flux $\left[\left(\left(\dot{m}(z)-\dot{m}(0)\right)/\dot{m}(0)\right)\times 100\right]$, is constant and (b) relative error for specific energy, $\left[\left(\left(\dot{E}(z)-\dot{E}(0)\right)/\dot{E}(0)\right)\times 100\right]$, is also constant from the bottom of the wellbore to the top.

Fig. 7 illustrates how the variables alter as the mixture flows up the production tubing. As expected, the expansion of the gas causes the vapour-phase density and the density of the mixture to decrease while the density of the liquid increases as the fluid flows up to the surface. To maintain a constant mass flow rate throughout the flow, the velocity increases as the temperature and pressure declines as the fluid flows upward. As the mixture flows up the tubing, there is condensation due to the cooling effects from temperature and pressure decline which makes the gas to be denser. This was affirmed by carrying out a sensitivity

analysis at lower temperatures and pressures as shown in Fig. 7. As can be seen in Fig. 7(e), the liquid density increases while the vapour density and the velocity decreases as the temperature declines from 185.6 K to 175 K.

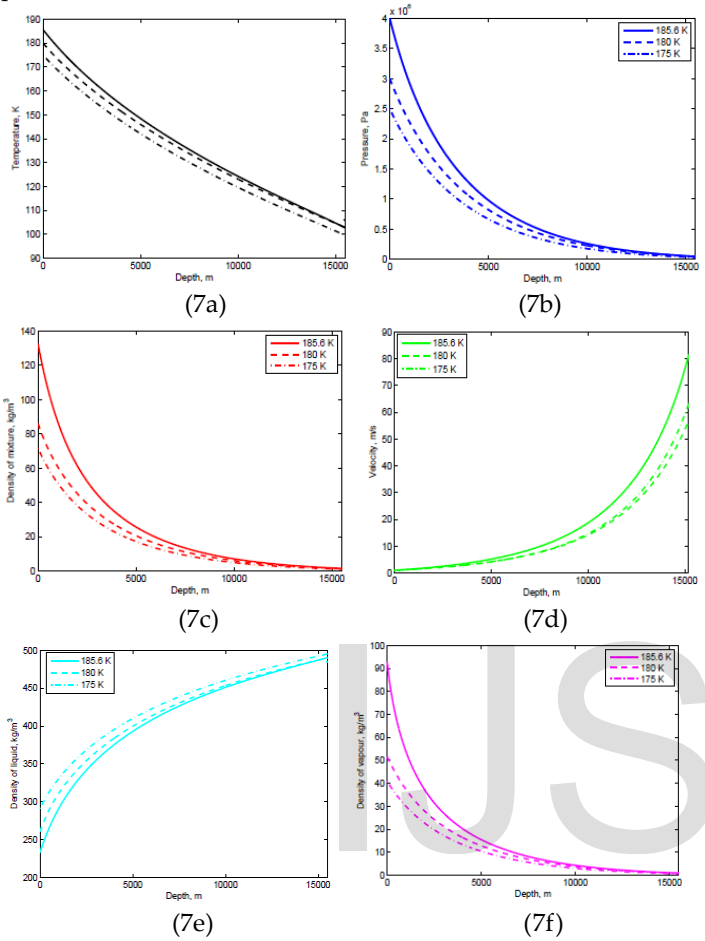

Fig. 7: typical flow profiles for pure methane undergoing phase change, showing (a) temperature, (b) pressure, (c) mixture density, (d) mixture velocity, (e) liquid density and (f) vapour density against depth.

The simulation of methane undergoing phase change was validated against data from NIST RefProp software, as shown in Fig. 8. Fig.s 8(a) and 8(b) are comparisons of the variation of the phase densities with temperature, while Fig.s 8(c) and 8(d) compare the phase densities against pressure. The density of the liquid decreases with increasing temperature and pressure while that of the vapour increases with increasing temperature and pressure. This is because at higher temperatures and pressures, vaporization takes place that increases the vapour density. This is explained thus: at higher temperatures and pressures, the tendency of the liquid molecules to change phase to vapour increases. In order to maintain equilibrium, the number of molecules escaping from the liquid phase to the vapour phase must be equal to the number of molecules returning. However, since at higher temperatures the molecules possess higher kinetic energy, the number of molecules escaping per second increases, saturating the vapour phase, thus increasing the number of vapour molecules in the vapour phase above the liquid. Conversely, as the temperature decreases, it takes less vapour to saturate the vapour phase, hence the decrease in the vapour density as the pressure and temperature decreases during flow.

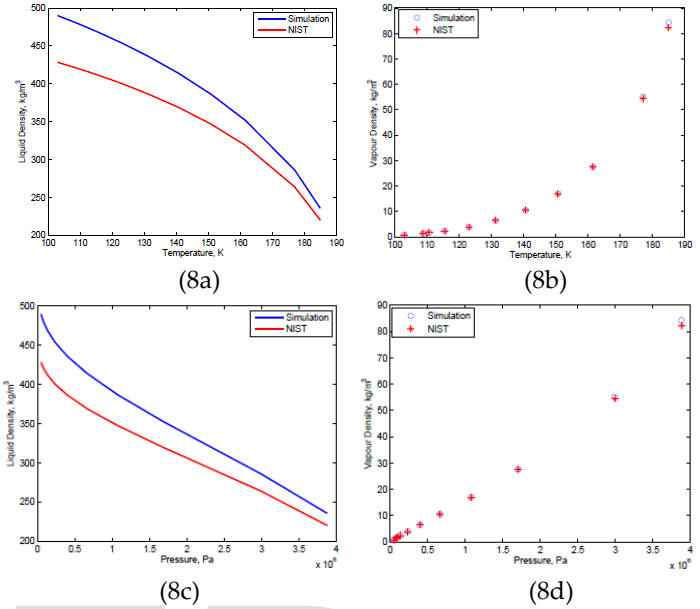

Fig. 8: Validation for pure methane undergoing phase change, showing (a) temperature versus liquid density, (b) temperature versus vapour density, (c) pressure versus liquid density and (d) pressure versus vapour density.

From Fig.s 8(b) and 8(d), the model results for the density of the vapour-phase are in very good agreement with the results from the NIST RefProp simulator. However, the prediction of the density of the liquid phase is not as close as shown in From Fig.s 8(a) and 8(c). This can be attributed to the inherent shortcomings associated with cubic equations of state which lack accuracy in the prediction of liquid properties (e.g liquid density) compared to the gas properties [9]. Although, the Peng-Robinson equation of state used in this paper, has been found to be one of the most accurate predictors of liquid density among many other cubic equations of state. Moreover, methane being the lightest hydrocarbon primarily exists in the vapour phase, and hence its vapour phase properties can be more accurately estimated than its liquid phase properties. The trends for the prediction of the liquid density from the model and the NIST RefProp software are consistent, and the values of the liquid density becomes similar at the bottom of the tubing where the temperature and pressure are higher.

5 CONCLUSION

The modelling of a single-component system is presented to understand the behaviour of a multicomponent natural gas mixture. The models were set up using the conservation of mass, momentum and energy equations, an equation of state (gas

laws or the Peng-Robinson cubic equation of state) and appropriate constitutive equations. A simple case of the flow of an ideal gas was first modelled, which was later modified to real gas flow and later real gas with and without phase change. At every stage of the numerical simulation, the temperature, pressure, density and velocity of the mixture was examined and the gas law and laws of conservation are checked to ensure that they are obeyed. Moreover, the results from these models were also validated using experimental data to ensure consistency. The results show good agreement with experimental data and quite promising in understanding liquid dropout during flow in gas wells.

Nomenclature

Symbol	Units	Description
a	$m^6Pa\ mol^{-2}$	Peng-Robinson EOS attractive parameter for mixture
A	-	Peng-Robinson EOS parameter
B	-	Peng-Robinson EOS parameter
b	$m^3\ mol^{-1}$	Peng-Robinson co-volume parameter
bm	$m^3\ mol^{-1}$	Peng-Robinson co-volume parameter for mixture
f	Pa	fugacity
g	m/s^2	acceleration due to gravity
H	Joules mol−1	enthalpy
M	kg	mass
m	kg	molecular mass
N	-	number of components
p	Pa	pressure
R	$m^3PaK^{-1}mol^{-1}$	gas Constant
R	$m^3Pa\ K^{-1}\ mol^{-1}kg^{-1}$	specific gas constant
T	K	temperature
v	m/s	velocity
V	$m^3\ mol^{-1}$	molar volume
x	-	mole fraction
Z	-	gas deviation factor
Greek symbols		
ω	-	acentric factor
σ	N/m^2	stress
ρ	kg/m^3	density
Superscripts		
v		vapour phase
l		liquid phase
Subscripts		
i,j,k		component index
m		mixture

References

[1] C.U. Ikoku. Natural Gas Production Engineering Handbook, Reprint Edition, Krieger Publishing Company, Malabar, Florida, USA, 1992

[2] T. Ahmed, reservoir Engineering Handbook, Second Edition, Gulf Professional Publishing, Boston, USA, 2001

[3] O. Bratland. Pipe Flow 1: single-phase flow assurance. www.bratland.com, 2009. Accessed March ,2021

[4] O. Bratland, Pipe Flow 2: single-phase flow assurance. www.bratland.com, 2010. Accessed March, 2021

[5] D.Y. Peng and D.B. Robinson. Anew two-constant equation of state. Ind.Eng. Chem. Fundam., 15(1), 59-64, 1976

[6] A.A. Fouad and L.L. Lloyd, Self-consistent equations for calculating the ideal gas heat capacity, enthalpy, and entrop. Fluid Phase Equilibria, 6(3-4): 169-179, 1981

[7] M.Adewumi, PNG 520: Phase relations in reservoir Engineering, College of Earth and Mineral Science, Pennsylvania State University, USA, https://.eeducation.psu.edu/png520/, 2014. Accessed 12 March, 2020

[8] U.Setzmann and W.Wagner, Anew equation of state and tables of thermodynamic properties for methane covering the range from the melting line to 625K at pressures up to 1000 MPa. J.Phy. Chem. Ref Data, 20(6): 1061-1155,1991

[9] K.H.Kumar and K.E. Starling. The most general density-cubic equation of state: application to pure nonpolar fluids. Ind. Eng. Chem. Fund., 21(3): 255-262, 1982.